doi:10.1093/brain/awz196 BRAIN 2019: 142; 2688–2704 | 2688

BRAIN
A JOURNAL OF NEUROLOGY

Stereoelectroencephalography: retrospective analysis of 742 procedures in a single centre

Francesco Cardinale,[1] Michele Rizzi,[1] Elena Vignati,[1] Massimo Cossu,[1] Laura Castana,[1] Piergiorgio d'Orio,[1,2] Martina Revay,[1,3] Martina Della Costanza,[1,4] Laura Tassi,[1] Roberto Mai,[1] Ivana Sartori,[1] Lino Nobili,[5] Francesca Gozzo,[1] Veronica Pelliccia,[1,6] Valeria Mariani,[1,7,8] Giorgio Lo Russo[1] and Stefano Francione[1]

This retrospective description of a surgical series is aimed at reporting on indications, methodology, results on seizures, outcome predictors and complications from a 20-year stereoelectroencephalography (SEEG) activity performed at a single epilepsy surgery centre. Prospectively collected data from a consecutive series of 742 SEEG procedures carried out on 713 patients were reviewed and described. Long-term seizure outcome of SEEG-guided resections was defined as a binomial variable: absence (ILAE classes 1–2) or recurrence (ILAE classes 3–6) of disabling seizures. Predictors of seizure outcome were analysed by preliminary uni/bivariate analyses followed by multivariate logistic regression. Furthermore, results on seizures of these subjects were compared with those obtained in 1128 patients operated on after only non-invasive evaluation. Survival analyses were also carried out, limited to patients with a minimum follow-up of 10 years. Resective surgery has been indicated for 570 patients (79.9%). Two-hundred and seventy-nine of 470 patients operated on (59.4%) were free of disabling seizures at least 2 years after resective surgery. Negative magnetic resonance and post-surgical lesion remnant were significant risk factors for seizure recurrence, while type II focal cortical dysplasia, balloon cells, glioneuronal tumours, hippocampal sclerosis, older age at epilepsy onset and periventricular nodular heterotopy were significantly associated with seizure freedom. Twenty-five of 153 patients who underwent radio-frequency thermal coagulation (16.3%) were optimal responders. Thirteen of 742 (1.8%) procedures were complicated by unexpected events, including three (0.4%) major complications and one fatality (0.1%). In conclusion, SEEG is a safe and efficient methodology for invasive definition of the epileptogenic zone in the most challenging patients. Despite the progressive increase of MRI-negative cases, the proportion of seizure-free patients did not decrease throughout the years.

1 'Claudio Munari' Centre for Epilepsy Surgery, ASST GOM Niguarda, Milan, Italy
2 Neuroscience Institute, CNR, Parma, Italy
3 Neurosurgery Residency Program, University of Milan, Milan, Italy
4 Neurosurgery Unit, Polytechnic, University of Marche, Ancona, Italy
5 Child Neuropsychiatry Unit, IRCCS 'G. Gaslini' Institute, DINOGMI, University of Genoa, Genoa, Italy
6 Department of Neuroscience, University of Parma, Parma, Italy
7 Department of Neuroradiology, IRCCS Mondino Foundation, Pavia, Italy
8 Department of Biomedical and Neuromotor Sciences, University of Bologna, Bologna, Italy

Correspondence to: Michele Rizzi, MD
'Claudio Munari' Centre for Epilepsy Surgery, ASST Grande Ospedale Metropolitano Niguarda, Piazza Ospedale Maggiore, 3 - 20162, Milano, Italy
E-mail: michele.rizzi@ospedaleniguarda.it

Keywords: epilepsy surgery; SEEG; drug-resistant focal epilepsy; seizure outcome; prognostic factors

Abbreviations: 3DIRA = 3D imaging and robotic assistance; FCD = focal cortical dysplasia; RF-THC = radio-frequency thermal coagulation; SEEG = stereoelectroencephalography

Received November 11, 2018. Revised April 24, 2019. Accepted May 6, 2019. Advance Access publication July 15, 2019

Introduction

Surgery has been demonstrated as an effective option for the treatment of drug-resistant focal epilepsy (Wiebe *et al.*, 2001; Dwivedi *et al.*, 2017). Epilepsy surgery is based on the epileptogenic zone concept, defined as 'the site of the beginning and of primary organization of the epileptic seizures' (Munari and Bancaud, 1985). Intracranial EEG is necessary to identify the epileptogenic zone in 25–50% of subjects with drug-resistant focal epilepsy (Cossu *et al.*, 2005). Intracerebral electrodes enable direct recording from almost every cerebral structure, including gyral crowns, bottom of sulci and white matter. Stereoelectroencephalography (SEEG) was developed at Hôpital Sainte Anne, Paris, as a method for epileptogenic zone definition by means of intracerebral electrodes (Bancaud and Talairach, 1965). This method spread to many other centres in France and also to a few in Italy, Switzerland, Canada and South America, but its application at other epilepsy surgery programmes was limited for a long time. The late spread of the SEEG method can be explained highlighting the different concepts supporting the term 'epileptogenic zone'. Bancaud and Talairach 'emphasized the existence of fast synchronizing discharges that might involve a single region, or distinct but interconnected regions' (Chauvel, 2001), leading to the above-reported definition of the epileptogenic zone (Munari and Bancaud, 1985). This concept of a network organization, mainly based on SEEG evidence, was different from the more popular one, mainly surgery-driven, that led to a definition of the epileptogenic zone as 'the minimum amount of cortex that must be resected (inactivated or completely disconnected) to produce seizure freedom' (Carreno and Lüders, 2001). The French-school 'network vision of epilepsy' has recently been summarized, illustrated and exhaustively discussed by the Marseille team (Bartolomei *et al.*, 2017). The SEEG method spread very late also because of the technical complexity of electrode implantation (Gonzalez-Martinez *et al.*, 2014). In the last decade, improvements in neuroimaging, image-guided surgery and robotics have made SEEG more accessible (Cardinale *et al.*, 2016; Joswig *et al.*, 2018).

The goal of this study is to describe our 20-year-long SEEG activity, reporting on indications, surgical technique, results on seizures, outcome predictors and complications. To the best of our knowledge, this is the largest SEEG series ever reported.

Material and methods

Data collection

This retrospective analysis of a surgical series was based on our prospectively maintained database. All patients or their guardians gave their informed consent. The local Ethical Committee approved this study in 2014.

Populations

Depending on specific purposes, different subsets of patients were examined:

SEEG713

Efficacy (number of SEEG studied patients/number of SEEG studied and operated on patients), and morbidity of SEEG were analysed in a population of 713 patients (SEEG713) who underwent SEEG between May 1996 and July 2018.

SEEG630

A subset of 630 patients (SEEG630) who underwent SEEG up to July 2016 was analysed searching for predictors of seizure outcome (minimum follow-up = 24 months), by means of multivariate analysis. Three further subsets were considered as follows:

SURG470

A subset of 470 patients (SURG470) who underwent SEEG-guided resective/disconnective surgery.

SURG278

A subset of 278 patients (SURG278) who underwent SEEG-guided resective/disconnective surgery with at least 10 years of follow-up.

RF-THC153

A subset of 153 patients (RF-THC153) who underwent SEEG-guided radio-frequency thermal coagulation (RF-THC).

SURG1851

The population of 1851 patients (SURG1851) who underwent resective/disconnective surgery up to July 2018 was analysed to report on indications to SEEG.

SURG1598

A subset of 1598 patients (SURG1598) who underwent resective/disconnective surgery with a minimum follow-up of 24 months was analysed to compare seizure results between subjects who were, or were not, studied with SEEG, by means of contingency table analysis.

SURG767

A subset of 767 patients (SURG767, including SURG278) who underwent resective/disconnective surgery with at least 10 years of follow-up was analysed to test if the chance of being free of disabling seizures was different between subjects who were, or were not, studied with SEEG, adjusting for time (Kaplan-Meier curves and Log-Rank test).

Non-invasive workup

All patients underwent clinical history collection, neurological examination, MRI and neuropsychological evaluation. MRI datasets were obtained with Philips 1.5 T scanners throughout the analysed period. Gyroscan, Gyroscan NT and Achieva NT were the scanner models used in the periods 1996–1999, 2000–2005 and 2006–2018, respectively. Non-invasive video-EEG (VEEG) monitoring was carried out in most SEEG-studied patients. Over the last 5 years, several

MRI datasets were processed with the surface-projected fluid attenuation inversion recovery (SUPR-FLAIR) technique for statistical surface-based analysis of cortical hyperintensities (Cardinale *et al.*, 2017*a*). Interictal PET with 2-deoxy-2-[fluorine-18]fluoro-D-glucose integrated with CT (^{18}F-FDG PET/CT) and electrical source imaging (ESI) based on high density EEG (HD-EEG) recordings were introduced to our workflow 8 and 3 years ago, respectively.

When the epileptogenic zone was not localized, SEEG was indicated with the following main goals (Kahane *et al.*, 2006): demonstrating that brain regions suspected to be the epileptogenic zone show the expected ictal pattern; considering if this pattern reflects propagation of an ictal discharge generated elsewhere; delineating the border of the epileptogenic zone 'precisely', to perform the minimum cortical resection; assessing whether the resection will be possible or not (likely relationship with eloquent cortex); evaluating the relationship between an anatomical lesion and the epileptogenic zone; and considering the possibility of intraprocedural RF-THC.

Surgical methodology

The traditional Talairach technique included two surgical steps, the so-called 'repérage' (i.e. the multimodal topographical mapping of the structures and regions of interest, classically obtained by means of stereoscopic ventriculography and angiography, and then progressively incorporating more modern image modalities) and the electrode implantation (Cossu *et al.*, 2005). This workflow, although progressively updated, was in use at our centre until 2009. Since then, we moved toward a one-step surgical technique. The watershed consisted of the adoption of an image-guided surgery workflow fully based on 3D Imaging and Robotic Assistance (3DIRA).

Planning and implantation steps of 3DIRA workflow were detailed previously (Cardinale *et al.*, 2013, 2015, 2017*b*) and are briefly summarized below.

Image acquisition

All patients were imaged by brain 3D MRI and 3D cone beam CT digital subtraction angiography (3D CBCT DSA) in frameless and marker-less conditions, days or weeks before implantation. MRI datasets were obtained according to previously published recommendations (Colombo *et al.*, 2012). We used the O-arm 1000 System (Medtronic) to obtain high resolution images to be processed for brain vasculature segmentation and visualization.

Image processing

Image datasets were processed mainly with FSL (Jenkinson *et al.*, 2012), Freesurfer (Fischl, 2012), 3D Slicer (Fedorov *et al.*, 2012) and SEEGA (Narizzano *et al.*, 2017). At the end of the pipeline, processed data were loaded into the stereotactic planning software.

Trajectory planning

Stereotactic trajectories were planned with Voxim (Renishaw Mayfield SA). Entry points and target points were defined for each trajectory by inspecting multiplanar reconstructions, brain and vasculature surface rendering, and images reformatted according to the planned vector.

Electrode implantation

Electrodes (8924 Microdeep Intracerebral Electrodes-D08, Dixi Medical; 1160 Depth Electrodes Range 2069, Alcis) were implanted under general anaesthesia. A single dose of antibiotics was administered preoperatively. Until 2016, the patient's head was registered to the robotic space in frame-based conditions with specific localizers visible at 2D X-rays. From 2016, we introduced the use of Neurolocate™, a frameless and touchless registration tool providing a better accuracy profile (Cardinale *et al.*, 2017*b*). Once image space is registered to the stereotactic workspace, the robot (Neuromate®, Renishaw Mayfield SA) aligns the tool holder along the vector of each planned trajectory. For each trajectory, the skull is drilled (2.1 mm) and a hollow screw is advanced through the bone. Once all the guiding screws are fixed, the frame is removed and the electrodes are placed under radioscopic control. Finally, a 3D CBCT is obtained with the O-arm to verify the electrode positioning.

Radio-frequency thermal coagulation

When indicated, RF-THCs were carried out prior to electrode removal (Cossu *et al.*, 2015). In most cases, larger ablations were obtained by progressively and slowly increasing the power up to ~8 W, as suggested previously (Bourdillon *et al.*, 2016).

Electrode removal

At the end of VEEG monitoring, electrodes were removed at the patient's bedside. Local anaesthesia and skin stitches are no longer used, and sedation is used only in non-cooperative patients.

Definitions

We defined cumulative results on seizures (i.e. assessed at the last available outcome) as 'favourable' when matching criteria for International League Against Epilepsy (ILAE) classes 1 and 2 (Wieser *et al.*, 2001), corresponding to Engel classes Ia–Ic (Engel *et al.*, 1993). Conversely, outcome was considered as 'unfavourable' when patients were not free of disabling seizures at the last available outcome (ILAE classes 3–6, Engel classes II–IV).

We defined 'complication' as any deviation from the normal postoperative course when: (i) a surgical treatment was adopted; (ii) an unexpected new neurological deficit lasting > 3 months was observed; (iii) the event led to the abortion of the clinical programme; (iv) a potentially life-threatening event (including intracranial infections or status epilepticus) occurred; or (v) the patient died.

A complication was defined as 'major' when a permanent organ dysfunction or death occurred.

We defined 'notable event' as any deviation from the normal postoperative course when none of the above listed criteria were matched.

We defined 'RF-THC optimal responders' as those patients who had (i) a favourable outcome; or (ii) were not keen to undergo resective/disconnective surgery because they were satisfied with clinical results (whatever the outcome class), in both cases after a minimum follow-up of 24 months.

Variables and statistical analysis

Seizure outcome was assessed as specified above. Statistical analysis was carried out to investigate the risk of postoperative seizures in patients who underwent resective/disconnective surgery, categorized as a dichotomous variable: absence (ILAE classes 1–2) or recurrence (ILAE classes 3–6) of disabling seizures. The dichotomy was different for the outcome variable of RF-THC: optimal responder or not. Several explanatory variables were considered for uni/bivariate and multivariate analysis (Table 2 and Supplementary Tables 2–5).

Uni/bivariate analysis was propaedeutic, and the subsequent multivariate regression analysis was carried out to identify risk factors for seizure recurrence. Kruskal-Wallis rank sum test was used to analyse numerical variables, and Fisher's two-tailed exact test was carried out for categorical variables. Uni/bivariate analysis was used only as a preliminary inspection.

A 'multivariate logistic regression model was fitted to assess the association of the explanatory variables with the outcome. Explanatory variables were selected with a multistep process, fitting some preliminary models and a final 'best' model. All variables potentially associated with the outcome (*P*-value at uni/bivariate analysis < 0.25) were sequentially added to the model, one by one, and their relevance in explaining independently the variability of the outcome was judged. After the best model was fitted, relative risk was calculated with the technique of Zhang and Yu (1998).

Furthermore, Kaplan-Meier curves were plotted and a Log-Rank test was carried out to compare results on seizures for 10-years follow-up of SEEG-studied patients versus the others (SURG767). A Cox proportional hazards regression model was also fitted to assess the association of the explanatory variables with the outcome, adjusting for time in the subgroup SURG278.

Linear regression analyses were carried out to study changes over time of numerical variables.

$P < 0.05$ was considered significant. *P*-values between 0.05 and 0.1 were considered as trend towards significance. Statistical analysis was carried out using R 3.4.0. An illustrative case was included in the study.

Data availability

The data that support the findings of this study are available from the corresponding author, upon reasonable request.

Results

SEEG713

This group included 400 males and 313 females, mean age ± standard deviation (SD) = 26.2 ± 11.8 years (range: 2–56). One hundred and eighty-five patients (25.9%) were younger than 18. Twenty-nine patients were investigated twice, for a total of 742 procedures with 10 084 electrodes. The mean number ± SD of electrodes per implantation was 13.59 ± 2.63 (range: 3–22), with an increasing trend throughout the years (Fig. 1A). Less than six electrodes were implanted in only six procedures, including five perilesional investigations carried out in early years, and one procedure aborted for technical issues.

Six hundred and one (84%) of 713 subjects were investigated unilaterally, 87 (12%) had an asymmetric bilateral study and 25 (4%) a symmetric bilateral one (Fig. 1B). 3DIRA workflow was used in 323 out of 742 implantations (43.5%). Six hundred and sixty-eight of 713 (93.6%) patients preliminarily underwent non-invasive long-term VEEG monitoring. Of the 45 patients who did not undergo preliminary non-invasive VEEG monitoring, 11 had a recorded seizure during standard EEG examination, and 34 had an MRI-visible lesion seated in a position coherent with clinical history, ictal semiology and interictal EEG. Of the latter 34 patients, four had a periventricular nodular heterotopy (PNH); two had a polymicrogyria (PMG); 13 had tumoral, malformative or post-ischaemic lesions seated in eloquent areas; 13 had malformative or post-ischaemic lesions quite well visible at MRI but with blurred contours; the remaining two had previous resections of cortical malformations followed by a period of seizure freedom and then by seizure relapse.

After SEEG, resective/disconnective surgery was indicated for 570 patients (79.9%), and 524 of these were operated on. One hundred and thirty-six patients were excluded from any subsequent surgery because the epileptogenic zone was not defined, or was multifocal, or included eloquent cortical areas (Fig. 1C). See Supplementary Fig. 1 for further details on SEEG efficacy.

Complications

Thirteen of 742 (1.8%) procedures were complicated, including four (0.5%) major events: one death from massive brain oedema following severe hyponatraemia, two permanent contralateral hemiplegic conditions due to intracerebral bleeding, one unilateral leg compartment syndrome resulting in mild permanent deficit of foot dorsal flexion (Table 1).

The overall complication rate was lower with 3DIRA workflow compared with the traditional procedure, even if not significantly (0.9% versus 2.4%, $P = 0.16$). Of

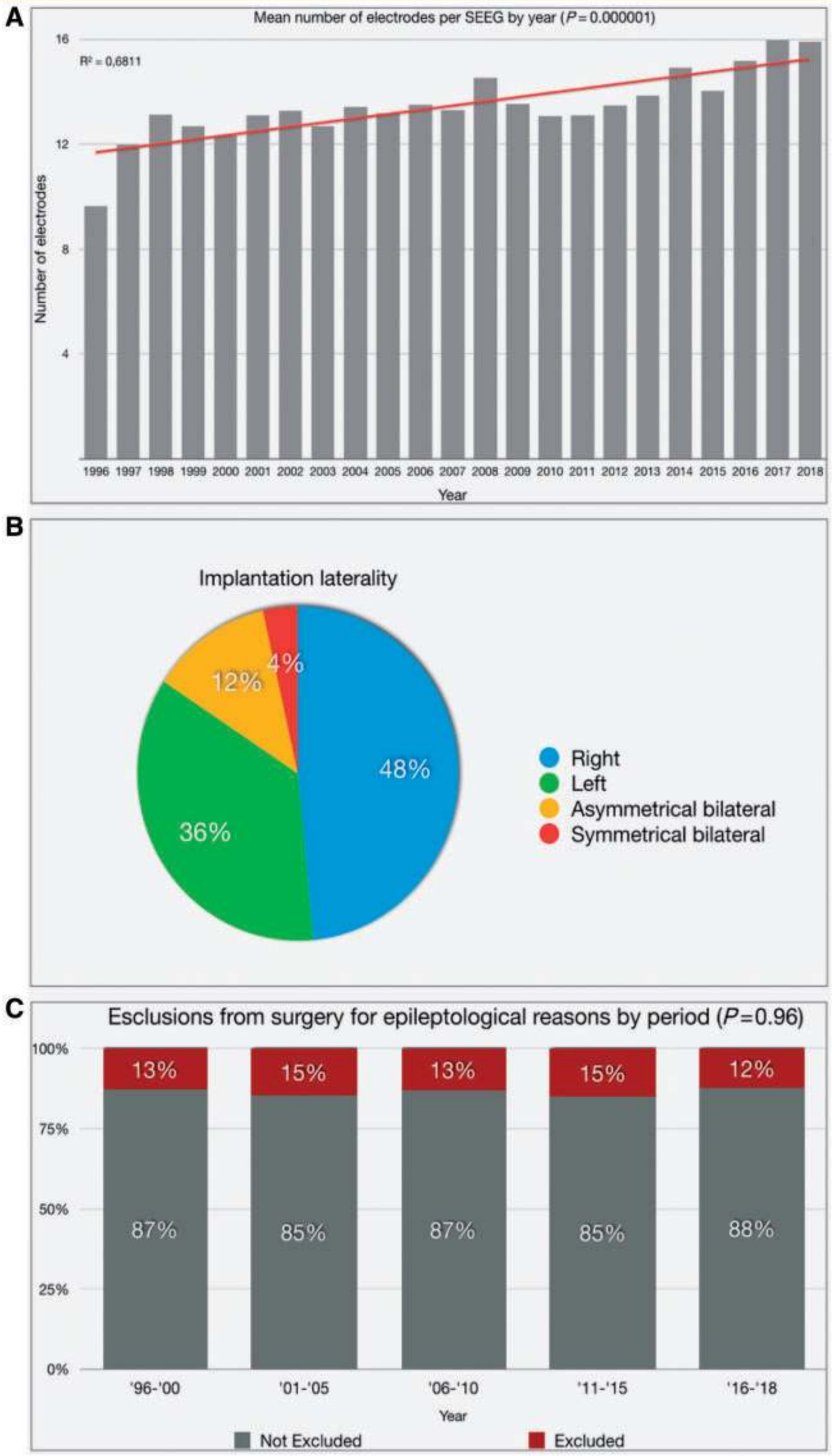

Figure 1 Synthetic report of SEEG activity: part 1. (**A**) Bar chart of mean number of electrodes implanted per SEEG by year, with tendency line. The number of electrodes per procedure significantly increased by the years. (**B**) Pie chart of implantation laterality: 84% of SEEG implantations were unilateral. (**C**) Proportions of exclusions from surgery for epileptological reasons following SEEG, by periods. About 15% of patients were not offered a resective/disconnective surgery because the epileptogenic zone was not defined, or was multifocal, or included eloquent cortical areas.

note, no major procedure-related complication occurred with 3DIRA (5181 implanted electrodes). In particular, none of the major bleedings occurred with the new workflow. All implantation-related intracranial bleedings occurred at the cortical entry point. The overall observed rate of clinically relevant intracranial bleedings for electrode was 4/10 084 (0.04%), including three intraparenchymal haemorrhages and a subdural one.

Table 1 Complications of SEEG and RF-THC, listed in order of occurrence

Patient ID	Event	Grading	Permanent injury	Surgery	Year	Workflow	Phase	Causation
SEEG								
343	Epidural haematoma	Minor	No	Clot removal	1996	Traditional	Framed angiography	Spec.
595	Intracerebral haematoma	Major	Hemiplegia	Clot removal	1998	Traditional	Electrode implantation	Spec.
42	Intracerebral haematoma	Minor	No	Clot removal	2000	Traditional	Electrode implantation	Spec.
288	Retained broken electrode	Minor	No	Electrode removal	2000	Traditional	SEEG monitoring	Spec.
386	Hydrocephalus	Minor	No	Yes	2001	Traditional	Electrode removal	Spec.
181	Brain abscess	Minor	No	No	2001	Traditional	Electrode implantation	Spec.
1807	Intracerebral haematoma	Major	Hemiplegia	Clot removal	2002	Traditional	Electrode implantation	Spec.
1788	Subdural acute haematoma	Minor	No	Clot removal	2003	Traditional	Electrode implantation	Spec.
2492	Lung atelectasis	Minor	No	No	2005	Traditional	Electrode implantation	Gen.
3014	Death (severe hyponatraemia and massive brain oedema)	Major	Death	No	2007	Traditional	Electrode implantation	Gen.
3595	Status epilepticus (with small IC clot after electrode removal)	Minor	No	Anticipated electrode removal	2011	3DIRA	SEEG monitoring	Spec.
4384	Leg compartment syndrome	Major	Mild deficit of foot dorsal flexion	Fasciotomy	2013	3DIRA	Electrode implantation	Gen.
1040	Internal carotid artery dissection	Minor	No	No	2015	3DIRA	Angiography	Spec.
RF-THC								
3839	Intracranial haemorrhage with visual field defect	Major	Subquadrantic visual field defect	No	2012	3DIRA	THC	Spec.
4419	Ablation causing a dominant-side parietal syndrome	Major	Complex neuropsychological disorder	No	2013	3DIRA	THC	Spec.
5143	Ablation causing haemianopia	Major	Subquadrantic visual field defect	No	2017	3DIRA	THC	Spec.

Gen. = related to the general perioperative management; IC = intra-cerebral; RF-THC = radio frequency thermal coagulation; Spec. = related to the specific neurosurgical procedure.

Other notable events, not classified as complications, are reported Supplementary Table 1. They included asymptomatic intracranial bleedings, aseptic encephalitis, leg deep venous thrombosis, psychotic attack, retained broken electrode, electrode displacement, transient mild motor deficit, allergic reaction to contrast medium at angiography, and pneumocephalus at electrode removal.

SURG470

Two-hundred and seventy-nine patients (59.4%) had a favourable outcome, while disabling seizures recurred in the remaining 191 (40.6%) (mean follow-up ± SD = 140.5 ± 67.7 months). In particular, 230 (48.9%) were in ILAE class 1 at last follow-up ($n = 184$ Engel Ia and $n = 46$ Engel Ic). The percentage of seizure-free patients increased throughout the analysed period, although this trend was not significant (Fig. 2C). Thirty-two patients experienced some ictal events during the follow-up period, but then returned to be free of disabling seizures.

The variable list and the results of uni/bivariate analysis are reported in Supplementary Tables 2 and 3. At multivariate logistic regression analysis (Table 2), negative MRI and remnant lesion independently predicted unfavourable outcome, while type II focal cortical dysplasia (FCD), balloon cells and glioneuronal tumours at histology, hippocampal sclerosis and PNH at MRI, and older age at epilepsy onset independently predicted favourable outcome.

SURG278

At multivariate survival analysis (Table 2), negative MRI and remnant lesion independently predicted unfavourable outcome, while type II FCD independently predicted favourable outcome. See Table 2 for the variables that were maintained in the model because of a trend towards significance.

RF-THC153

Twenty-five patients (16.3%) were optimal responders (20 out of 25 in ILAE classes 1–2), while results were unsatisfactory for the remaining 128 (83.7%) (mean follow-up ± SD = 74 ± 26.4 months). In detail, 15 patients out of the 25 were in ILAE class 1 at last follow-up ($n = 11$ Engel class Ia, $n = 4$

Table 2 Output of fitted multivariate models

Logistic regression models									
Variable	**Category**	**Reference category**	**Coeff**	**SE**	**OR**	**95% CI_{or}**	**RR**	**95% CI_{rr}**	***P*-value**
SURG470									
MRI	Negative	Positive	0.76	0.24	2.14	1.34 3.45	1.32	1.13 1.49	0.002*
Balloon cells at histology	Yes	No	−1.49	0.49	0.23	0.08 0.57	0.25	0.09 0.60	0.002*
FCD type II at histology	Yes	No	−0.91	0.31	0.40	0.22 0.72	0.46	0.27 0.77	0.003*
GN tumours at histology	Yes	No	−1.27	0.42	0.28	0.12 0.62	0.34	0.15 0.69	0.003*
HS evidence at MRI	Yes	No	−1.30	0.46	0.27	0.10 0.64	0.31	0.12 0.69	0.005*
Post-surgical lesion remnant	Yes	No	0.82	0.30	2.26	1.26 4.11	1.40	1.12 1.63	0.007*
Age at epilepsy onset			−0.04	0.02	0.96	0.93 0.99	NA	NA NA	0.014*
PNH at MRI	Yes	No	−1.22	0.56	0.29	0.09 0.84	0.35	0.12 0.88	0.030*
THC153									
PNH at MRI	Yes	No	−3.25	0.68	0.04	0.01 0.14	0.06	0.01 0.20	0.000002*
Sex	Male	Female	−1.03	0.55	0.36	0.11 1.01	0.73	0.37 1.00	0.06[a]
Seizure frequency	Monthly	Rare	2.26	1.53	9.58	0.48 302.39	1.21	0.83 1.23	0.14
	Weekly		2.88	1.47	17.84	1.02 513.13	1.18	1.00 1.19	0.049*
	Daily		2.32	1.46	10.18	0.57 287.34	1.13	0.91 1.15	0.11
Cox regression model									
Variable	**Category**	**Reference category**	**Coeff**	**SE**	**HR**	**95% CI_{hr}**	**RR**	**95% CI_{rr}**	***P*-value**
SURG278									
MRI	Negative	Positive	0.57	0.18	1.76	1.25 2.49	NA	NA NA	0.001*
FCD type II at histology	Yes	No	−0.90	0.32	0.41	0.22 0.76	NA	NA NA	0.005*
Balloon cells at histology	Yes	No	−0.84	0.45	0.43	0.18 1.05	NA	NA NA	0.065[a]
GN tumours at histology	Yes	No	−0.49	0.29	0.61	0.35 1.08	NA	NA NA	0.088[a]
HS evidence at MRI	Yes	No	−0.65	0.34	0.52	0.27 1.02	NA	NA NA	0.057[a]

Output of fitted multivariate models: SURG470 (outcome variable = seizure recurrence); THC153 (outcome variable = treatment failure); SURG278 (censoring event = first disabling seizure).

CI = confidence interval; Coeff = coefficient; FCD = focal cortical dysplasia; GN = glioneuronal tumours; HR = hazard ratio; HS = hippocampal sclerosis; NA = not available; OR = odds ratio; PNH = periventricular nodular heterotopy; RR = relative risk; SE = standard error.

*Statistically significant.

[a]Trend towards significance.

Engel class Ic), five were in ILAE class 2, and the remaining five were in ILAE class 3. All of these five ILAE 3 patients expressed their willingness to undergo resective/disconnective surgery if their satisfaction decreased. The variable list and the results of uni/bivariate analysis are reported in Supplementary Tables 4 and 5. At multivariate analysis (Table 2), higher seizure rate independently predicted unsatisfactory outcome (with significance for weekly seizures), while PNH at MRI was significantly associated with better outcome. Sex was also included in the model because male gender resulted in a better outcome with a trend towards significance.

Complications

Three procedures (2%) were complicated by major events (one complex neuropsychological disorder and two subquadrantic visual field defects). Other notable events (transient

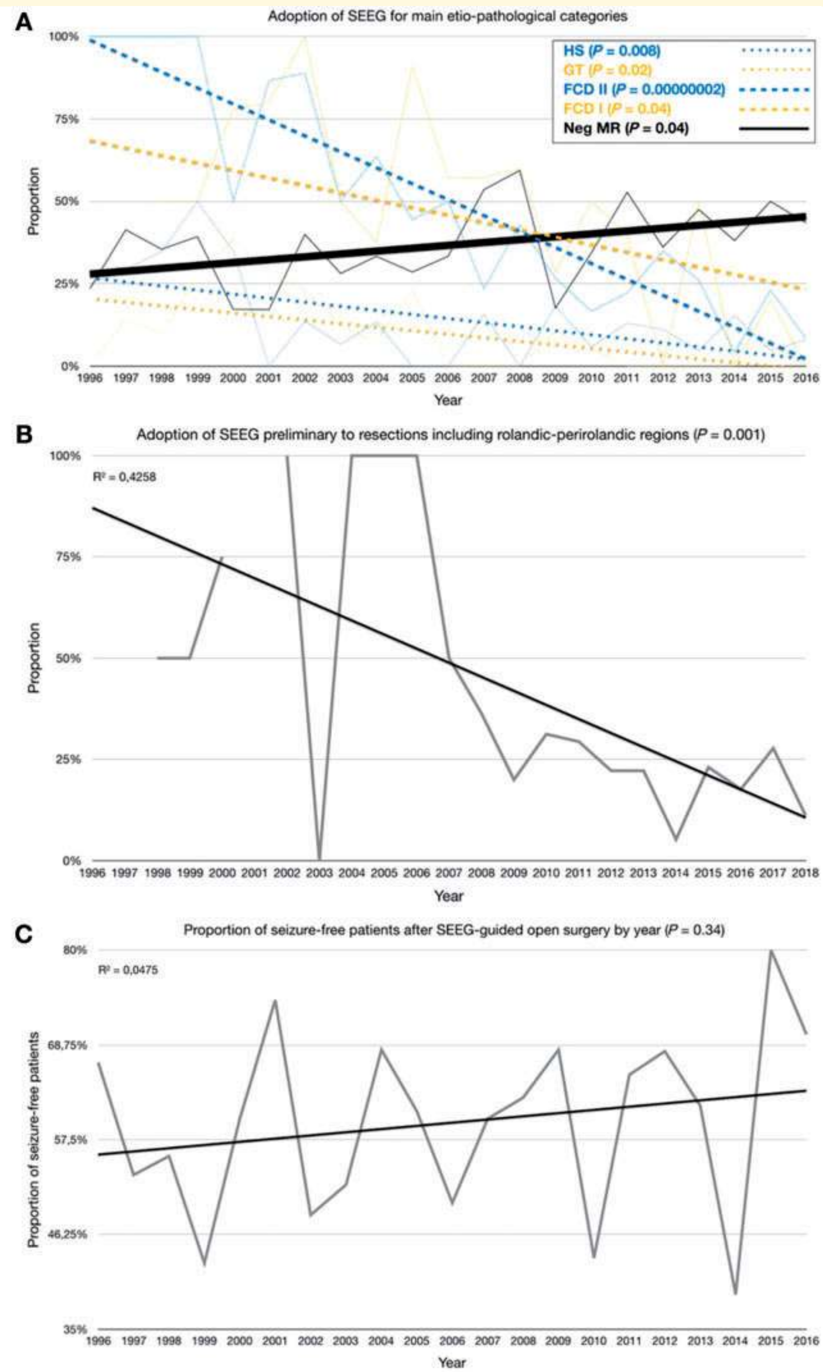

Figure 2 Synthetic report of SEEG activity: part 2. (**A**) Adoption of SEEG for main aetiopathological categories, by year, with tendency lines. The number of SEEG performed in MRI-negative patients significantly increased with time. (**B**) Adoption of SEEG preliminary to resections including rolandic-prerolandic regions significantly decreased with time. (**C**) Proportion of seizure-free patients after SEEG-guided open surgery, by years, with regression line. Despite the progressive increase of MRI-negative patients, results on seizures did not get worse.

motor impairment, prolonged memory deficit, clinically relevant cerebral oedema), not classified as complications, are reported in Supplementary Table 1. Of note, one patient developed an expected and anticipated permanent contralateral motor deficit (Cossu *et al.*, 2015), not classified as a complication.

SURG1851

Throughout the years, the bulk of MRI-negative SEEG-studied subjects progressively increased, while the proportion of SEEG-studied patients suffering from the most common aetiopathological categories (hippocampal sclerosis, glioneuronal tumours, type I and type II FCD) significantly decreased (Fig. 2A). Nonetheless, some of the latter patients still underwent SEEG in the later years. As an example, in the last 18 months of the analysed period, we performed SEEG in 11 of 38 type II FCD patients, who were subsequently operated on.

The proportion of SEEG-studied patients who underwent resective surgery in the rolandic-perirolandic region progressively and significantly decreased ($P = 0.001$) (Fig. 2B).

SURG1598

After resective/disconnective surgery, disabling seizures recurred (ILAE classes 3–6) in 191 of 470 patients (40.6%) who underwent SEEG, and in 207 of 1128 patients (18.4%) who were operated on after non-invasive investigations only ($P < 2.2^{-16}$).

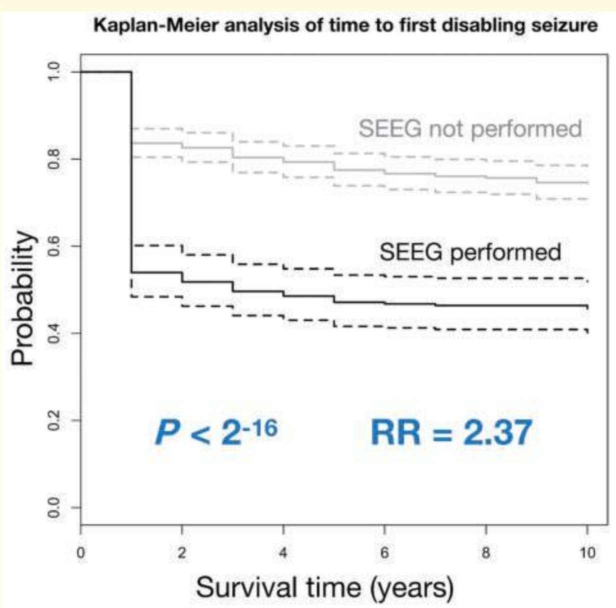

Figure 3 Kaplan-Meier analysis of time to first disabling seizure. Censoring events were assessed yearly, at outpatient visits, approximating the time of occurrence accordingly. Log-Rank test confirmed that the chance of seizure recurrence is significantly more than double (relative risk, RR = 2.37) for patients who underwent SEEG. Of note, most relapses occurred in the first post-surgical year.

SURG767

The chance of recurrence of disabling seizures (ILAE classes 3–6) was more than double for patients who underwent SEEG, as illustrated in Fig. 3 (relative risk = 2.37, $P < 2.2^{-16}$).

Illustrative case

The patient, a right-handed male, first had seizures at the age of 12, with impaired awareness followed by bilateral tonic phenomena, or right limb jerks. He was referred to our centre 3 years later because of drug resistance, and reported monthly seizures with aphasia, followed by right head deviation and right clonic movements. He also had daily episodes of anomia and 'mind numbness'. Interictal EEG showed left epileptiform activity with posterior temporal prevalence. Epileptogenic zone localization was hypothesized in the left temporo-parieto-occipital region and SEEG was indicated because of non-invasive work-up findings (Fig. 4A–G) and for lack of any MRI-visible abnormalities (Fig. 6B and Supplementary Fig. 2). Fifteen intracerebral electrodes were implanted (Fig. 4H and I), and VEEG monitoring lasted 11 days.

Based on SEEG findings (Figs 5A–F and 6A), a temporobasal resection was carried out, with only a transient reading impairment. Histopathological examination showed gliosis. The patient is free from any seizures since surgery, and no longer taking any antiepileptic drugs (follow-up of 58 months). Cognitive evaluation showed a normal profile, including reading functions, 12 months after surgery.

Discussion

Indications and number of electrodes

SEEG is indicated when the analysis of anatomo-electro-clinical correlations does not allow a clear definition of epileptogenic zone and a consequent surgical proposal. Some particular situations have been advocated: regarding temporal lobe epilepsy, SEEG can be indicated

> 'when clinical and EEG data do not allow the existence of a mesial or neocortical temporal lobe generator to be ruled out,... when the combination of clinical data and presurgical investigations suggest the possibility of seizures arising independently from both TL ... in suspected pseudo-temporal lobe epilepsy when extra-temporal areas are involved early in the seizure according to non-invasive data' (Minotti *et al.*, 2018).

In extratemporal lobe epilepsies, SEEG is essentially indicated in MRI-negative patients and 'in the case of discordance between the topography of the lesion and the ictal clinical data, to define the respective roles of the lesion, the EZ and the eloquent cortex' (Minotti *et al.*, 2018). Indications changed progressively throughout the years in

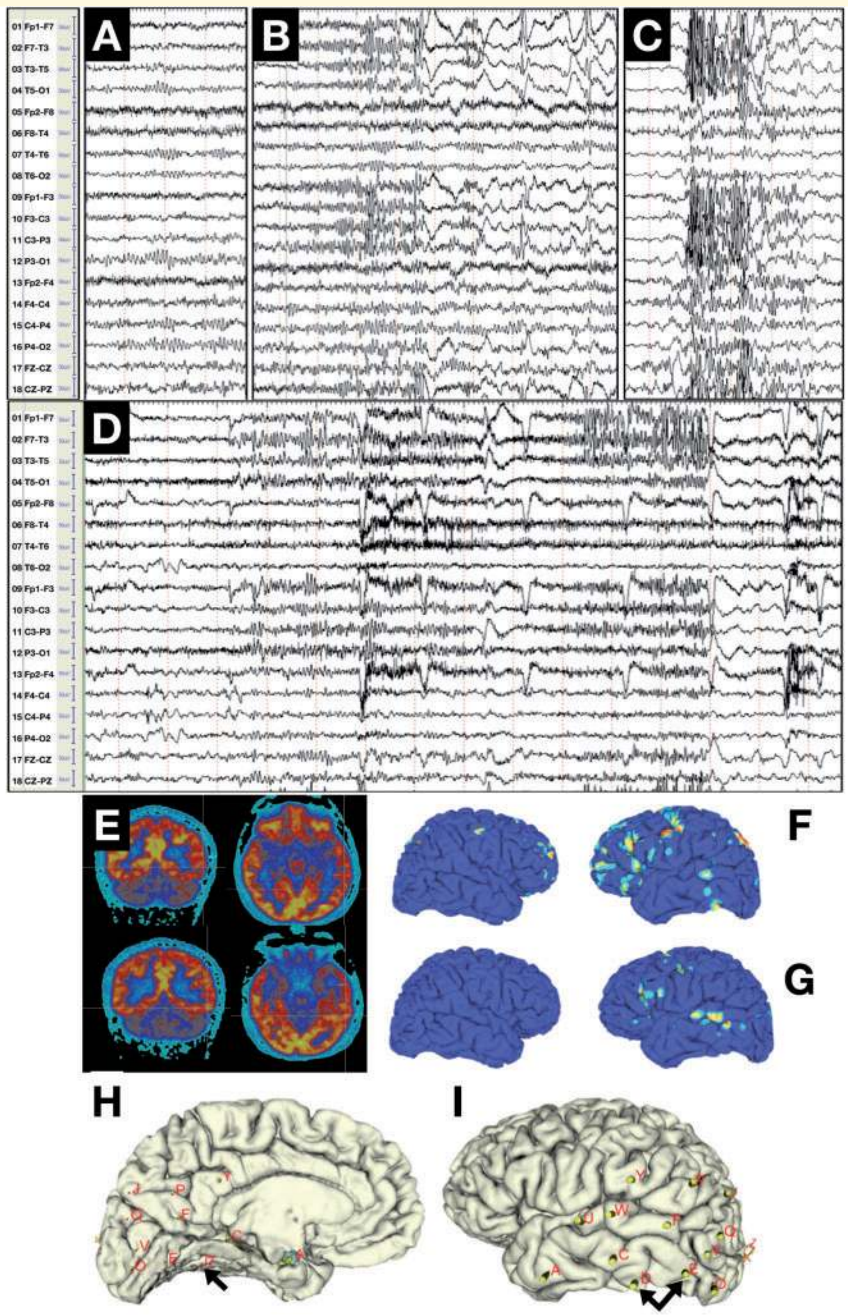

Figure 4 Illustrative case: non-invasive work-up and SEEG implantation. (**A**) Interictal basal EEG: eyes closed with normal and symmetrical background activity. (**B**) Hyperventilation: burst of recruiting rhythmic activity in beta band, evolving in a sequence of spike-and-waves. Both activities selectively involve the left hemisphere with a posterior prevalence and rapid rhythm on T3–T5. (**C**) Nap: burst of very high amplitude poly-spikes, spread out over the left hemisphere. (**D**) Ictal EEG correlate of a typical subjective manifestation, later described as 'mind numbness', and bilateral blinks. It is characterized by flattening of the traces over the left hemisphere, more evident on T3–T5, followed by a mid-amplitude rhythmic activity evolving over the next 5 s and then becoming faster, mainly on left posterior regions. (**E**) Interictal ^{18}F-FDG PET, depicting hypometabolism of the lateral part of the left temporo-parieto-occipital region. Language functional MRI: surface mapping of activations related to verbal fluency (**F**) and naming by verbal description (**G**) tasks administration. Both paradigms demonstrate left hemispheric dominance for the language. SEEG implantation: 3D rendering of the post-implantation scene, with mesial (**H**) and lateral (**I**) views. Arrows indicate the contacts of electrodes D and E recording from the core of the epileptogenic zone.

our experience. The use of SEEG progressively decreased in patients with MRI-visible lesions, with a parallel increase of MRI-negative cases. Different factors can justify such evolution at our centre. The evidence that lesions such as FCDs (Chassoux *et al.*, 2000; Lo Russo *et al.*, 2003; Tassi *et al.*, 2012) or glioneuronal tumours (Aubert *et al.*, 2009; Chassoux *et al.*, 2013) are intrinsically highly epileptogenic led us to resect them without any invasive investigations, at least when it was possible to contour them well on MRI images and when their position was concordant with

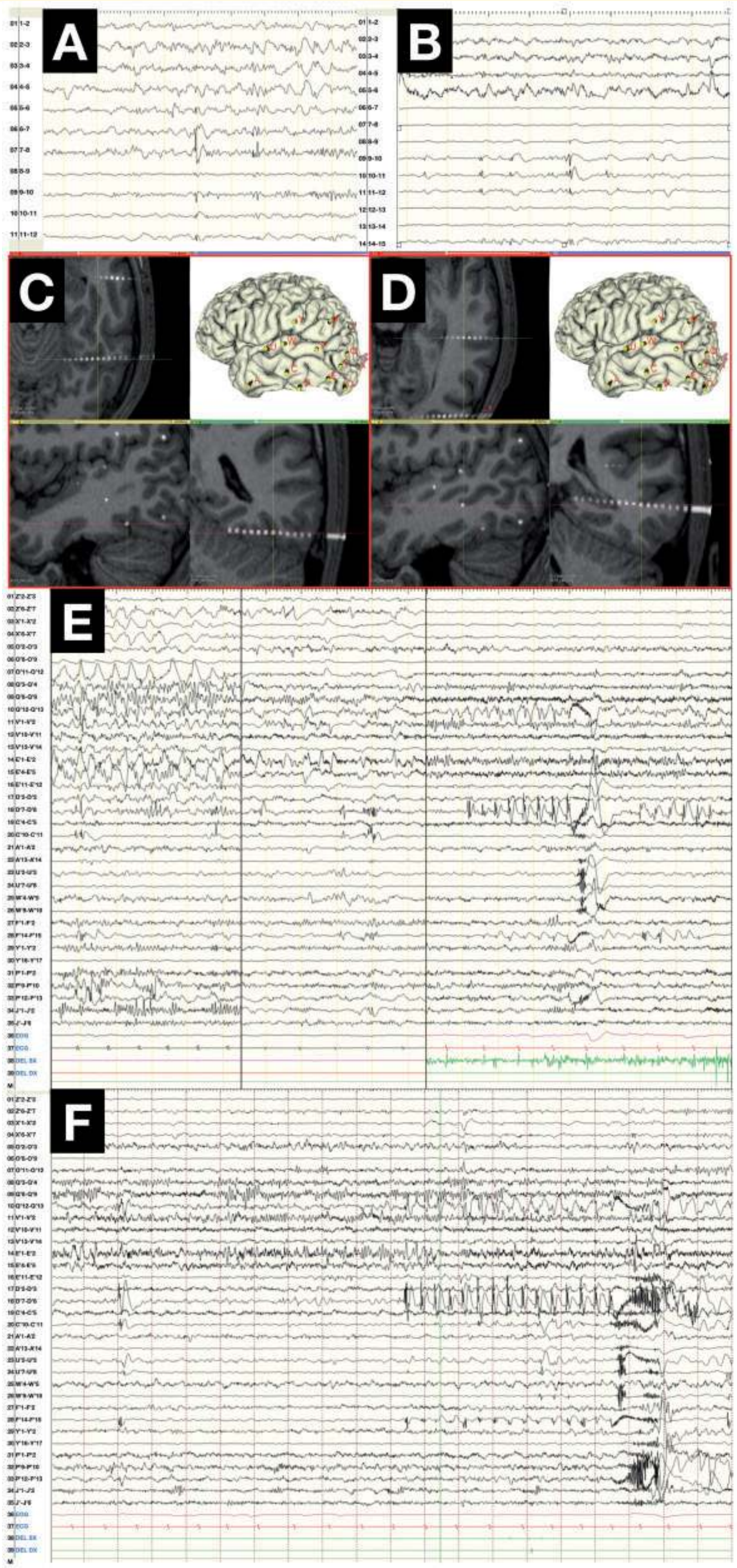

Figure 5 Illustrative case: SEEG findings (part 1). (**A**) Traces recorded from contacts 1–5 of electrode D show low amplitude β-rhythms superimposed to a slow activity. Leads 7–10 of electrode D, seated in the inferior temporal gyrus (ITG) and in the temporo-occipital sulcus, recorded a beta rhythm intermixed with very fast spikes and bursts of pathological low voltage fast activity, possible markers of dysplastic tissue. (**B**) Traces recorded from leads 2–5 of electrode C show normal activity from posterior hippocampus. Leads 9–11 of electrode C (recording from the grey matter at the bottom of the superior temporal sulcus) recorded a clear burst of low amplitude fast activity, ending with recruiting modality and a fast spike. Leads 14–15 of electrode C (seated in the middle temporal gyrus, MTG) recorded an α-rhythm with rare slow spikes,

(continued)

electroclinical findings. Even when MRI-visible lesions were seated in the rolandic region, we preferred using intraoperative brain mapping or monitoring and 3D multimodal imaging. As highlighted previously, 3D reconstructions can help in delineating gyral and sulcal patterns and thus better understanding the convoluted brain anatomy for surgical planning (Cardinale *et al.*, 2015; Nowell *et al.*, 2015). It must, however, be emphasized that sometimes some dysplastic tissue is also seated beyond the contours of the MRI-visible abnormality, and this is true especially when a type FCD is suspected. In such cases, SEEG is advisable.

The mean number of electrodes per investigation at our centre is higher than elsewhere, even if comparable to the mean values reported by the groups from Lyon, Grenoble, Paris (Fondation Rothschild) and Cleveland Clinic Foundation (Cardinale *et al.*, 2016). The number of electrodes per patient, however, did not predict the seizure results in our study (Supplementary Table 3).

We can postulate that the evolution of SEEG indications and the increasing number of implanted electrodes per patient are due to similar reasons. Reluctance to consider MRI-negative cases for surgery was progressively mitigated by evidence of epilepsy-related focal abnormalities provided by novel diagnostic tools, including ^{18}FDG-PET/CT, 7 T brain magnetic resonance (Zucca *et al.*, 2016) SUPR-FLAIR statistical analysis, HD-EEG, and connectivity studies, which have been introduced and used with increasing frequency in the presurgical evaluation of the more difficult cases. These tools frequently provide additional working hypotheses, thus expanding the areas to be covered with intracerebral electrodes. Moreover, detailed reconstruction of convoluted brain anatomy often leads to local higher densities of implantation because attention is paid to abnormalities or variants of gyral and sulcal pattern. On the other hand, availability of image-guided, robot-assisted procedures has increased the accuracy of targeting and improved the safety profile of electrode implantations, making the surgeon more confident with more demanding cases requiring a high number of electrodes.

SEEG laterality

Gonzalez-Martinez *et al.* (2014) considered the possibility to lateralize the epileptogenic zone by means of bilateral implantation as one of the SEEG mainstays. A retrospective series of 184 patients who underwent bilateral SEEG has recently been published by the same group (Steriade *et al.*, 2018). The authors reported a 32% postoperative seizure-free rate, with a mean follow-up of 3.1 years. Moreover, they highlighted that only 58% of such bilateral SEEG-studied patients had a final surgery (resection or ablation), compared to 75–87% of non-selected SEEG cohorts previously published at Cleveland Clinic or elsewhere. The complexity of bilaterally-investigated patients can explain the lower rate of both the indications to final surgery and seizure freedom. They reported multifocality as the main reason for the higher contraindication rate to surgery. As suggested by the attention has to be paid to the 'non-invasive heralds of multifocality' to enhance the diagnostic accuracy of the pre-SEEG triage. The lower rate of seizure-free patients in the bilateral-SEEG population can reflect the epileptological features of this population. In fact, the 'electroclinical features unifocal epilepsy increase the odds of seizure freedom'.

In our series, only 16% of SEEG studies were bilateral, and only one-quarter of them symmetric, while the remaining three-quarters included only a few sentinel electrodes contralateral to the side of the main epileptogenic zone hypothesis (Fig. 1B). Overall, 80% of the patients were selected for surgery, with ~15% of patients not selected for any subsequent treatment (the remaining patients, ~5%, refused the final treatment option or were not operated on because of SEEG-related complications). Such a difference could be interpreted with a different attitude in indicating SEEG. Likely, most patients with supposed bilateral epileptogenic zone or with a weak hypothesis of unilateral focality are not offered invasive recordings at our centre. This peculiar aspect should be further investigated in the future, studying the large population of all patients who were admitted to any type of presurgical evaluation.

Planning and surgical workflow

Our image processing pipeline guaranteed not only an excellent safety profile, but it also provided us with 3D multimodal reconstructions that are helpful to assess where EEG activities are generated, to discuss SEEG findings at

Figure 5 Continued
synchronous with those of contacts 9–11. (**C** and **D**) 3D reconstruction of the pial surface with SEEG electrode models, and multiplanar superimposing of electrodes D and C after co-registration of preoperative 3D T_1-weighted MRI and post-implantation cone beam CT. Multiplanar reconstructions are centred on lead 7 of electrode D (**C**), and on lead 10 of electrode C (**D**). (**E**) Interictal activities with synthetic montage. *Left*: The EEG shows the restricted topography of fast spikes and burst, involving only D7–8 and C10–11. The occipital derivations (electrodes O, X and Z) show a delta activity. *Middle*: Pathological electrical activities, when faster, also involve other neocortical structures, such as the posterior superior temporal gyrus (STG) at the level of F14–15. *Right*: Sequence of spikes-and-waves with increasing rhythmicity localized on D7–8, with a limited propagation to F14–15 and a slow component to Q12–13. The burst of very fast activity following the rhythmic spike-and-wave sequence shows a larger topography with the involvement of U7–8, W4–5, W9–10, F14–15, Q12–13 and P12–13. (**F**) Typical episode of 'mind numbness', with a single spike-and-wave complex localized over D7–8, C10–11 and F14–15, involving also the superior occipital gyrus (Q12–13), the middle STG (U7–8) and the posterior insula (U2–3). After this abnormality, no clear ictal discharge is visible for ~8 min. Subsequently, a rhythmic spike-and-wave discharge starts, mainly over the ITG with a propagation similar to that described in (**E**), then ending with low voltage fast discharge involving also the posterior ITG (E11–12) and the anterior MTG (A13–14). Clinically, the patient was blinking fast. At the end of the discharge, he had only a typical sensation of numbness and speech difficulties.

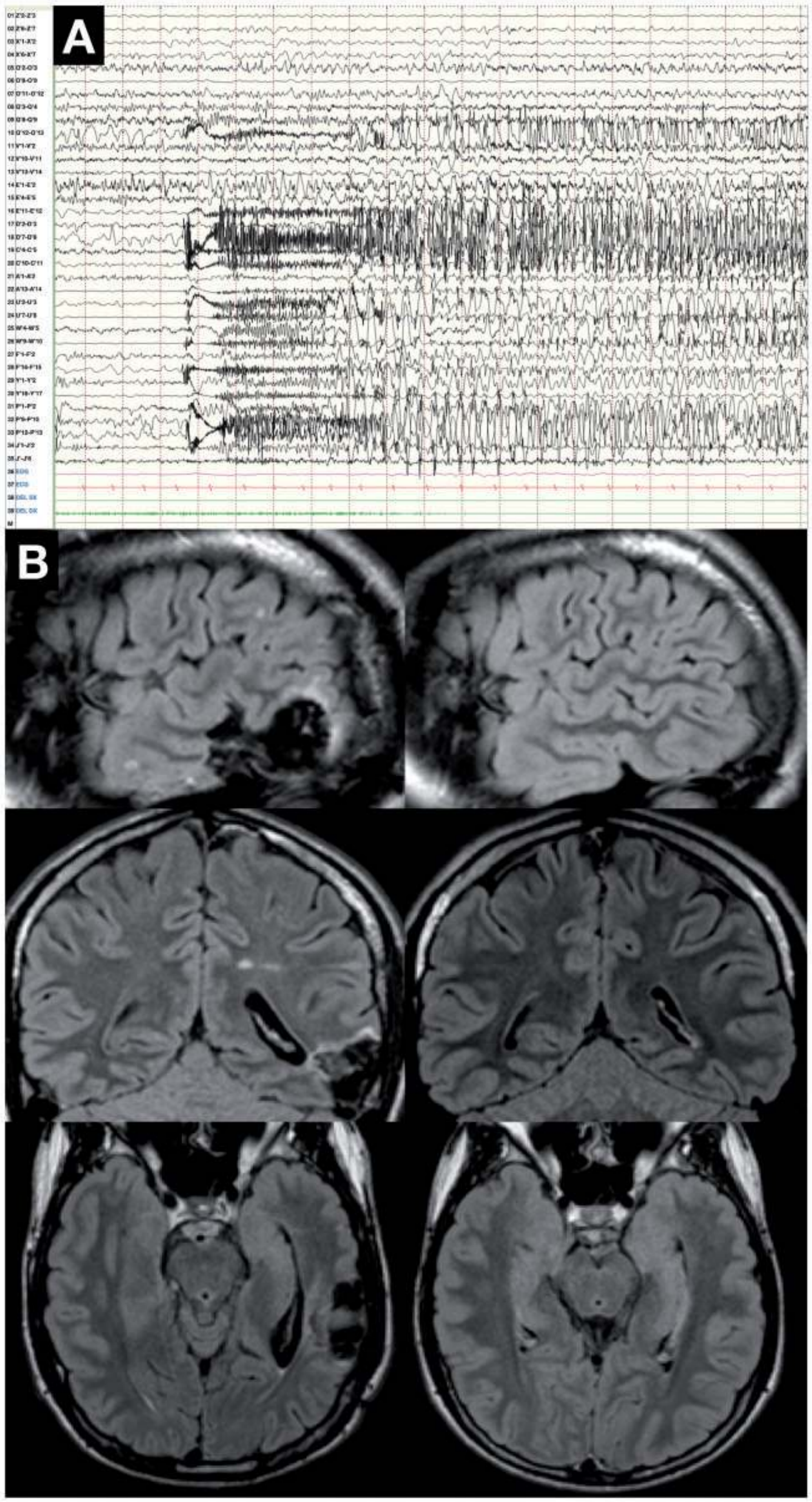

Figure 6 Illustrative case: SEEG findings (part 2) and postoperative MRI compared to the preoperative MRI. (**A**) Initial electrical correlate of a typical seizure. During neuropsychological testing, the ictal discharge starts and the patient immediately stops reading. The patient stares, with some movements of the head, seemingly following the observer. Six seconds later, also minimal movements stop and staring lasts 4 min. He gets relaxed at the end of this period, swallows and follows the observer, then is aphasic for > 5 min. The ictal discharge starts abruptly with a burst of mid-amplitude fast activity, localized from the beginning in the ITG and in other neocortical structures of the temporal lobe (superior temporal sulcus, STG, anterior MTG), anterior occipital (SOG) and inferior parietal regions. The fast activity lasts 1 min, then the discharge evolves with a burst of mid-amplitude spikes of 4 s before becoming a rhythmic discharge lasting for the remaining 4 min of the episode. All these modifications are driven by the ITG discharge, which is predominant all along the fit. After the spontaneous seizures recording,

(continued)

multidisciplinary conference and to optimize resective/disconnective surgery planning (Fig. 4I). Moreover, intraoperative visual comparison of multimodal scenes and surgical field mitigates the problem of navigation inaccuracies caused by brain shift (Harput *et al.*, 2014; Cardinale *et al.*, 2015). Direct recognition of patient-specific anatomy guarantees an optimal localization of surface and sulci even when brain is distorted by ongoing resection.

Stereotactic accuracy is crucial to avoid intracranial bleedings. We previously reported lower localization errors of implantation with 3DIRA workflow versus the traditional one, both at entry and target point (Cardinale *et al.*, 2013). A recent meta-analysis demonstrated that our accuracy at the cortical entry point (the most important risk zone) was the best ever reported (Vakharia *et al.*, 2017). Further accuracy improvements were determined by using the Neurolocate^{TM}, a new frameless and touchless registration tool optimized for the robotic assistant in use at our centre (Cardinale *et al.*, 2017*b*). According to multivariate analyses reported in our previous studies, we can state that such high accuracy profile mainly results from the combination of high resolution planning images and robotic assistance.

Seizure results

Resective/disconnective surgery

Despite the higher complexity of SEEG-studied cases, seizure results were favourable for 59.4% of patients who underwent resective/disconnective surgery, overall. Notwithstanding the progressive increase of the proportion of MRI-negative patients, seizure outcome did not worsen (Fig. 2C). Such results are comparable to those reported by another recent large series (González-Martínez *et al.*, 2016).

Not surprisingly, seizure outcome is better ($P < 2^{-16}$) in patients who underwent resective/disconnective surgery without any prior invasive recordings (Table 2 and Fig 3). This can be explained considering that SEEG is indicated in the most challenging, often MRI-negative cases.

SEEG-guided RF-THC was pioneered by the Lyon group (Guénot *et al.*, 2004). Since then, this technique has gained popularity in Europe. Bourdillon *et al.* (2017) reported 7% Engel class I after a 12-month minimum follow-up of a series of 162 patients. Our results were detailed in a previous study (Cossu *et al.*, 2015). In the present study, we confirmed that RF-THC is safe and feasible, with 20 patients (13.1%) in ILAE classes 1–2 after long-term follow-up. Moreover, an additional five patients (3.3%) were classified as optimal responders, even though they were not free of disabling seizures (ILAE class 3), suggesting a satisfying palliation.

Outcome predictors

Multivariate logistic regression analysis revealed several outcome predictors for patients who underwent SEEG-guided resective surgery: histological diagnosis of glioneuronal tumours, type II FCD, presence of balloon cells, and MRI evidence of hippocampal sclerosis or PNH reduced the risk of seizure recurrence at least by half. Similarly, older age at onset reduced the odds of unfavourable outcome. On the contrary, negative MRI and lesion remnant increased the risk of seizure recurrence by at least one-third (Table 2). Such findings are coherent with several previous studies on outcome predictors in general epilepsy surgery series, although the predictive value of MRI findings was found to be not significant in a series of 100 SEEG-studied patients (McGonigal *et al.*, 2007). The overall proportion of patients in ILAE classes 1–2 after surgery in Marseille was 57%, with both 1- and 2-year follow-ups, thus comparable to the results of the present report for SEEG-studied patients (59% in ILAE classes 1–2, with a mean follow-up >11 years). Their 1-year follow-up results were even better with MRI-negative patients than with MRI-positive patients (ILAE classes 1–2 in 65% and 53% patients, respectively), while our results were poorer for MRI-negative patients than for MRI-positive patients (ILAE classes 1–2 in 46% and 67% patients, respectively).

We also carried out a survival analysis fitting a Cox model with very long-term outcome patients (SURG278). Some of the explanatory variables included in the logistic regression model were confirmed as significantly associated with seizure outcome (negative MRI and type II FCD), or at least showed a trend to significance (presence of balloon cells, MRI evidence of hippocampal sclerosis and histological diagnosis of glioneuronal tumours). On the contrary, significant association was not confirmed for PNH, older age at onset and lesion remnant (Table 2). These different findings can be explained with the smaller sample size used for survival analysis, determining a lower power of statistical testing. As the study was retrospective and follow-up was assessed only yearly at outpatient clinics, we limited

Figure 6 Continued
intracerebral stimulations at low (1 Hz) and high (50 Hz) frequency are carried out. Low frequency stimulations did not induce any ictal signs. High frequency 3 mA stimulations of W8–9 (seated at the STG) induced impairment of verbal comprehension, thus confirming left dominance for the language. No effects were obtained stimulating F14–15. The stimulation of the intermediate fusiform gyrus (D2–3) allowed us to reproduce a seizure, and was associated with a discharge almost identical to the spontaneous ones, prevalent on the anterior ITG and neocortical structures. (**B**) Postoperative multiplanar T_2-weighted FLAIR MRI images (*left*) showing the resected region, compared to preoperative images (*right*). More detailed FLAIR thin slices, cut at the region of interest, are provided in Supplementary Fig. 2.

this analysis to the subgroup of patients who had a minimum follow-up of 10 years, similar to the study published by de Tisi and co-workers (2011). Survival analysis allowed us to adjust our findings for time-to-first-disabling-seizure. Nonetheless, it must also be considered that this kind of analysis is not fully optimal for epilepsy data, characterized by recurrent ictal episodes and by the possibility of multiple switching between the status of seizure-free and not seizure-free, in both directions (Jeong *et al.*, 2005). In fact, 32 of the 151 SEEG-studied patients who were censored in our survival analysis were free of disabling seizures 10 years after surgery. This could be explained by admitting the possibility that these patients became drug-responsive, and post-surgical optimization of the pharmacological treatment was then successful. Furthermore, considering that three of these patients have been drug-free for several years and are still seizure-free, a running-down phenomenon could be also advocated.

Logistic regression analysis for patients who underwent RF-THC confirmed that PNH is the best indication for such an ablation technique (Table 2). This evidence is in line with the indications proposed on the basis of a recent meta-analysis:

> 'The first indication concerns patients in whom a SEEG is required to determine whether surgery is feasible and in whom resection is indeed possible. Even if surgery is performed owing to insufficient efficacy of SEEG-guided RF-THC, the procedure remains interesting owing to its high positive predictive value for good outcome after surgery. The second indication concerns patients in whom phase I non-invasive investigations have concluded to surgical contraindication and who may still undergo SEEG in a purely therapeutic perspective (small deep zones inaccessible to surgery and network nodes of large epileptic networks). Lastly, SEEG-guided RF-THC can be considered as a first-line treatment for periventricular nodular heterotopia' (Bourdillon *et al.*, 2019).

On the contrary, higher seizure frequency seems to be a negative predictor, as does female gender (Table 2). The interpretation of this last finding is not easy. Four of 5 optimal responders in ILAE class 3 are males. Thus, a different gender-related attitude in evaluating the impact of partial seizure suppression could be advocated. Larger sample size studies are needed to confirm this finding.

Complications

Because of the lack of a generally accepted classification and grading system of complications in neurosurgery (Ferroli *et al.*, 2015), we reclassified postoperative events that occurred in our series. As an example, in our previous report (Cardinale *et al.*, 2013), small and asymptomatic bleedings were considered as complications, at odds with general brain resective surgery. Thus, including such events could lead to an overestimation of clinically-relevant SEEG complication rate. Present criteria justify the difference with our previous papers. Nonetheless, we have listed all unusual events, both in the article and with more detail in the Supplementary material.

The present report confirmed that SEEG has an excellent safety profile (Table 1). Since introduction of the 3DIRA workflow, no major intracranial bleedings have occurred, testifying that new technologies and a rigorous approach have made this invasive procedure even safer than in the past. Despite the high number of intracranial electrodes, complications are relatively rare (Cardinale *et al.*, 2016; Mullin *et al.*, 2016), with a 0.04% rate of clinically-relevant intracranial bleedings per electrode in the present series.

As the rate of adverse events is generally low, it is difficult to analyse complication predictors. We believe that sub-millimetric accuracy is required to maintain the risk of intracranial bleeding as low as possible, especially at the cortical entry point. Such results have been obtained at our centre with a combination of tools, including high resolution planning images, appropriate processing, accurate intraoperative patient registration and robotic assistance.

The safety profile of RF-THC has also been found to be excellent in the present series, in agreement with previous reports (Cossu *et al.*, 2015; Bourdillon *et al.*, 2017; Dimova *et al.*, 2017).

Limitations of the study and future research

The most important limitation of our study is its retrospective design. Moreover, literature analysis was narrative and not systematic. It must also be highlighted that 3 T MRI scanners are not yet available at our hospital, thus limiting the external validity of our results regarding the predicting value of MRI findings.

Future efforts should be focused on increasing SEEG efficacy. Advanced image processing aimed at revealing subtle lesions or cortical areas interested by epileptogenic phenomena should also be extensively tested and validated.

Moreover, automatic planning of SEEG trajectories, which may contribute to reduction of man time, has been reported in preliminary studies (De Momi *et al.*, 2014; Scorza *et al.*, 2018), and our centre is engaged in further development and validation of this tool.

We can conclude that SEEG contributes to excellent results on seizures in the most challenging patients suffering from drug-resistant focal epilepsy, and its efficacy and safety profile justify the widespread of this methodology.

Acknowledgements

We would like to dedicate this work to the memory of Claudio Munari, our mentor, who guided us with his way of thinking and being, and of Barbara Ciniselli, our secretary, who assisted us daily with invaluable care and passion.

Funding

No funding was received towards this work.

Competing interests

F.C. was consultant (paid expert testimony) to Renishaw Mayfield, the manufacturer of Neuromate robotic system, until February 2019. M.R. is consultant to WISE srl, a start-up manufacturing implantable leads for neuromodulation and neuromonitoring.

Supplementary material

Supplementary material is available at *Brain* online.

References

Aubert S, Wendling F, Régis J, McGonigal A, Figarella-Branger D, Péragut JC, et al. Local and remote epileptogenicity in focal cortical dysplasias and neurodevelopmental tumours. Brain 2009; 132: 3072–86.

Bancaud J, Talairach J, editors. La Stéréo-ÉlectroEncéphaloGraphie dans l'épilepsie. Paris: Masson; 1965.

Bartolomei F, Lagarde S, Wendling F, McGonigal A, Jirsa V, Guye M, et al. Defining epileptogenic networks: contribution of SEEG and signal analysis. Epilepsia 2017; 58: 1131–47.

Bourdillon P, Isnard J, Catenoix H, Montavont A, Rheims S, Ryvlin P, et al. Stereo electro-encephalography-Guided Radiofrequency Thermocoagulation: from in vitro and in vivo data to technical guidelines. World Neurosurg 2016; 94: 73–9.

Bourdillon P, Isnard J, Catenoix H, Montavont A, Rheims S, Ryvlin P, et al. Stereo electroencephalography–guided radiofrequency thermocoagulation (SEEG-guided RF-TC) in drug-resistant focal epilepsy: Results from a 10-year experience. Epilepsia 2017; 58: 85–93.

Bourdillon P, Rheims S, Catenoix H, Montavont A, Ostrowsky K, Isnard J, et al. Surgical techniques: stereoelectroencephalography-guided radiofrequency-thermocoagulation (SEEG-guided RF-TC). Seizure 2019; Epub ahead of print. doi: 10.1016/j.seizure.2019.01.021.

Cardinale F, Cossu M, Castana L, Casaceli G, Schiariti MP, Miserocchi A, et al. Stereoelectroencephalography: surgical methodology, safety, and stereotactic application accuracy in 500 procedures. Neurosurgery 2013; 72: 353–66.

Cardinale F, Pero G, Quilici L, Piano M, Colombo P, Moscato A, et al. Cerebral angiography for multimodal surgical planning in epilepsy surgery: description of a new three-dimensional technique and literature review. World Neurosurg 2015; 84: 358–67.

Cardinale F, Casaceli G, Raneri F, Miller J, Lo Russo G. Implantation of stereoelectroencephalography electrodes: a systematic review. J Clin Neurophysiol 2016; 33: 490–502.

Cardinale F, Francione S, Gennari L, Citterio A, Sberna M, Tassi L, et al. SUrface-PRojected FLAIR (SUPR-FLAIR) analysis: a novel tool for advanced imaging of epilepsy. World Neurosurg 2017a; 98: 715–26.

Cardinale F, Rizzi M, D'Orio P, Casaceli G, Arnulfo G, Narizzano M, et al. A new tool for touch-free patient registration for robot-assisted intracranial surgery: application accuracy from a phantom study and a retrospective surgical series. Neurosurg Focus 2017b; 42: E8.

Carreno M, Lüders HO. General principles of presurgical evaluation. In: Lüders HO, Comair YG, editors. Epilepsy surgery. Philadelphia: Lippincott, Williams & Wilkins; 2001. p. 185–200.

Chassoux F, Devaux B, Landré E, Turak B, Nataf F, Varlet P, et al. Stereoelectroencephalography in focal cortical dysplasia: a 3D approach to delineating the dysplastic cortex. Brain 2000; 123: 1733–51.

Chassoux F, Landré E, Mellerio C, Laschet J, Devaux B, Daumas-Duport C. Dysembryoplastic neuroepithelial tumors: epileptogenicity related to histologic subtypes. Clin Neurophysiol 2013; 124: 1068–78.

Chauvel P. Contributions of Jean Talairach and Jean Bancaud to epilepsy surgery. In: Lüders HO, Comair YG, editors. Epilepsy Surgery. Philadelphia: Lippincott Williams & Wilkins; 2001. p. 35–41.

Colombo N, Tassi L, Deleo F, Citterio A, Bramerio M, Mai R, et al. Focal cortical dysplasia type IIa and IIb: MRI aspects in 118 cases proven by histopathology. Neuroradiology 2012; 54: 1065–77.

Cossu M, Cardinale F, Castana L, Citterio A, Francione S, Tassi L, et al. Stereoelectroencephalography in the presurgical evaluation of focal epilepsy: a retrospective analysis of 215 procedures. Neurosurgery 2005; 57: 706–18.

Cossu M, Fuschillo D, Casaceli G, Pelliccia V, Castana L, Mai R, et al. Stereoelectroencephalography-guided radiofrequency thermocoagulation in the epileptogenic zone: a retrospective study on 89 cases. J Neurosurg 2015; 123: 1358–67.

De Momi E, Caborni C, Cardinale F, Casaceli G, Castana L, Cossu M, et al. Multi-trajectories automatic planner for StereoElectroEncephaloGraphy (SEEG). Int J Comput Assist Radiol Surg 2014; 9: 1087–97.

de Tisi J, Bell GS, Peacock JL, McEvoy AW, Harkness WF, Sander JW, et al. The long-term outcome of adult epilepsy surgery, patterns of seizure remission, and relapse: a cohort study. Lancet 2011; 378: 1388–95.

Dimova P, de Palma L, Job-Chapron AS, Minotti L, Hoffmann D, Kahane P. Radiofrequency thermocoagulation of the seizure-onset zone during stereoelectroencephalography. Epilepsia 2017; 58: 381–92.

Dwivedi R, Ramanujam B, Chandra PS, Sapra S, Gulati S, Kalaivani M, et al. Surgery for drug-resistant epilepsy in children. N Engl J Med 2017; 377: 1639–47.

Engel J Jr, Van Ness PC, Rasmussen TB, Ojemann LM. Outcome with respect to epileptic seizures. Second edition. In: Engel J Jr, editor. Surgical Treatment of the Epilepsies. New York: Raven Press, LTD; 1993. p. 609–21.

Fedorov A, Beichel R, Kalpathy-Cramer J, Finet J, Fillion-Robin JC, Pujol S, et al. 3D Slicer as an image computing platform for the Quantitative Imaging Network. Magn Reson Imaging 2012; 30: 1323–41.

Ferroli P, Caldiroli D, Leonardi M, Broggi M. Letter to the Editor: Complications in neurosurgery: the need for a common language. J Neurosurg 2015; 122: 983–4.

Fischl B. FreeSurfer. Neuroimage 2012; 62: 774–81.

González-Martínez J, Bulacio J, Thompson S, Gale J, Smithason S, Najm I, et al. Technique, results, and complications related to robot-assisted stereoelectroencephalography. Neurosurgery 2016; 78: 169–79.

Gonzalez-Martinez J, Mullin J, Vadera S, Bulacio J, Hughes G, Jones S, et al. Stereotactic placement of depth electrodes in medically intractable epilepsy. J Neurosurg 2014; 120: 639–44.

Guénot M, Isnard J, Ryvlin P, Fischer C, Sindou M. SEEG-guided RF Thermocoagulation of Epileptic Foci: Feasibility, Safety, and Preliminary Results. Epilepsia 2004; 45: 1368–74.

Harput M V, Gonzalez-Lopez P, Türe U. Three-dimensional reconstruction of the topographical cerebral surface anatomy for presurgical planning with free Osirix software. Neurosurgery 2014; 10: 426–35.

Jenkinson M, Beckmann CF, Behrens TEJ, Woolrich MW. FSL. Neuroimage 2012; 62: 782–90.

Jeong SW, Lee SK, Hong K, Kim K, Chung C-K, Kim H. Prognostic Factors for the Surgery for Mesial Temporal Lobe Epilepsy: Longitudinal Analysis. Epilepsia 2005; 46: 1273–9.

Joswig H, Steven DA, Parrent AG, MacDougall KW, Mirsattari SM, McLachlan RS, et al. Intracranial Electroencephalographic Monitoring: From Subdural to Depth Electrodes. Can J Neurol Sci. 2018; 45: 336–8.
Kahane P, Landré E, Minotti L, Francione S, Ryvlin P. The Bancaud and Talairach view on the epileptogenic zone: a working hypothesis. Epileptic Disord 2006; 8: S16–26.
Lo Russo G, Tassi L, Cossu M, Cardinale F, Mai RF, Castana L, et al. Focal cortical resection in malformations of cortical development. Epileptic Disord 2003; 5: S115–23.
Minotti L, Montavont A, Scholly J, Tyvaert L, Taussig D. Indications and limits of stereoelectroencephalography (SEEG). Neurophysiol Clin 2018; 48: 15–24.
McGonigal A, Bartolomei F, Régis J, Guye M, Gavaret M, Trébuchon A, et al. Stereoelectroencephalography in presurgical assessment of MRI-negative epilepsy. Brain 2007; 130: 3169–83.
Mullin JP, Shriver M, Alomar S, Najm I, Bulacio J, Chauvel P, et al. Is SEEG safe? A systematic review and meta-analysis of stereo-electro-encephalography-related complications. Epilepsia 2016; 57: 386–401.
Munari C, Bancaud J. The role of stereo-electro-encephalography (SEEG) in the evaluation of partial epileptic patients. In: Porter R, Morselli P, editors. The epilepsies. Bodmin: Butterworth & Co. (Publishers) Ltd; 1985. p. 267–306.
Narizzano M, Arnulfo G, Ricci S, Toselli B, Tisdall M, Canessa A, et al. SEEG assistant: a 3DSlicer extension to support epilepsy surgery. BMC Bioinform 2017; 18: 1–13.
Nowell M, Rodionov R, Zombori G, Sparks R, Winston G, Kinghorn J, et al. Utility of 3D multimodality imaging in the implantation of intracranial electrodes in epilepsy. Epilepsia 2015; 56: 403–13.
Scorza D, Amoroso G, Cortés C, Artetxe A, Bertelsen A, Rizzi M, et al. Experience-based SEEG planning: from retrospective data to automated electrode trajectories suggestions. Healthc Technol Lett 2018; 5: 167–71.
Steriade C, Martins W, Bulacio J, Morita-Sherman ME, Nair D, Gupta A, et al. Localization yield and seizure outcome in patients undergoing bilateral SEEG exploration. Epilepsia 2018; 60: 107–20.
Tassi L, Garbelli R, Colombo N, Bramerio M, Lo Russo G, Mai RF, et al. Electroclinical, MRI and surgical outcomes in 100 epileptic patients with type II FCD. Epileptic Disord 2012; 14: 257–66.
Vakharia VN, Sparks R, O'Keeffe AG, Rodionov R, Miserocchi A, McEvoy A, et al. Accuracy of intracranial electrode placement for stereoencephalography: a systematic review and meta-analysis. Epilepsia 2017; 58: 921–32.
Wiebe S, Blume WT, Girvin JP, Eliasziw M. A randomized, controlled trial of surgery for temporal-lobe epilepsy. N Engl J Med 2001; 345: 311–8.
Wieser HG, Blume WT, Fish DR, Goldensohn E, Hufnagel A, King D, et al. Proposal for a new classification of outcome with respect to epileptic seizures following epilepsy surgery. Epilepsia 2001; 42: 282–6.
Zhang J, Yu KF. What's the relative risk? A method of correcting the odds ratio in cohort studies of common outcomes. J Am Med Assoc 1998; 280: 1690–1.
Zucca I, Milesi G, Medici V, Tassi L, Didato G, Cardinale F,et al. Type II focal cortical dysplasia: Ex vivo 7T magnetic resonance imaging abnormalities and histopathological comparisons. Ann Neurol 2016; 79: 42–58.